

Real-time PID Adaptive Decoupled Controller Applied Over a DC-DC Multivariable Boost Converter

Maximiliano Bueno-Lopez, Eduardo Giraldo

Abstract—An embedded real-time PID adaptive controller is proposed for three boost converters connected to three LED strings. The voltage control of the LEDs can generate any Red-Green-Blue (RGB) combination in order to obtain a reference RGB color. The LED system control is implemented in real-time using an adaptive multivariable decoupled control, where the voltage tracking for each LED string is performed simultaneously using a boost converter. The adaptive controller is based on an online least squares recursive estimation method and a PID type 2 controller. The proposed adaptive controller is evaluated in simulation over a boost converter and in real-time over three boost converters using the BOOSTXL-C2KLED system and a LAUNCHXL-F28379D microcontroller from Texas Instruments. A detailed analysis is performed in terms of the tracking error, the duty cycle signal, and the current signal. This analysis is shown for the simulated boost converter and also for the multivariate decoupled controller in real-time.

Index Terms—Real-time, PID control, Boost converter, LED.

I. INTRODUCTION

THE light-emitting diode (LED) systems have been widely used for lighting application in almost every field [1], [2]. In [3], current regulators with adaptive voltage feedback control are considered, showing an advance in comparison with pulse-width modulation (PWM) driving control with constant current control schemes [4]. Several control schemes can be applied over DC-DC converters, as proposed in [5], where a feedback linearization approach is proposed over a Buck converter. In addition, in [6] a fractional order PI controller is applied over synchronous buck converter, or also in [7], an alternative PID structure is used for the design of a boost converter by considering settling time and steady-state error.

The methodologies based on adaptive control are standard approaches to designing a control system based on estimation. For example, in [8], a multivariable approach is applied over a microgrid where the system is identified and controlled simultaneously. In [9], a multivariable adaptive control approach is applied over a four-leg converter, where a recursive least square identification method is applied based on an ARMA structure. In [10], an adaptive strategy for

Manuscript received May 18, 2022; revised November 3, 2022. This work is funded by project no. 6-22-8 entitled "Identificación y control de sistemas multivariables interconectados a gran escala" by Universidad Tecnológica de Pereira, Pereira, Colombia.

Maximiliano Bueno-Lopez is an associate professor at the Department of Electronics, Instrumentation and Control, Universidad del Cauca, Popayán, Colombia. E-mail: mbuenol@unicauca.edu.co

Eduardo Giraldo is a Full Professor at the Department of Electrical Engineering, Universidad Tecnológica de Pereira, Pereira, Colombia. Research group in Automatic Control. E-mail: egiraldo@utp.edu.co.

identification is also applied over a multivariable system corresponding to a wastewater treatment plant, where a polynomial structure is selected for modeling the system's dynamics. In [11], an alternative approach for adaptive control is presented where the identification and control are simultaneously applied over an induction motor.

This work proposes an embedded real-time PID adaptive controller for three boost converters connected to three LED strings. The voltage control of the LEDs can generate any Red-Green-Blue (RGB) combination to obtain a reference RGB color. The LED system control is performed in real-time using an adaptive multivariable decoupled control. The voltage tracking for each LED string is performed simultaneously using a boost converter. The adaptive controller is based on an online least squares recursive estimation method and a PID type 2 controller. The proposed controller is evaluated both in simulation over a boost converter and in real-time over three boost converters using the BOOSTXL-C2KLED system and a LAUNCHXL C2000 F28379D microcontroller from Texas Instruments. A detailed analysis of tracking performance is presented for the embedded control. This article is organized as follows: in section II are presented the boost converter model and the adaptive multivariable PID type 2 controller. In section III are presented the obtained results for the proposed controller in simulation and in real time, and finally, in section IV are presented the conclusions and final remarks.

II. THEORETICAL FRAMEWORK

A. DC-DC Boost converter

In this work, three DC-DC boost converters are simultaneously controlled for voltage tracking. Each of the boost converters can be considered as a simplified model of the DC-DC boost converter proposed in [12]. This simplified model is presented in Fig. 1.

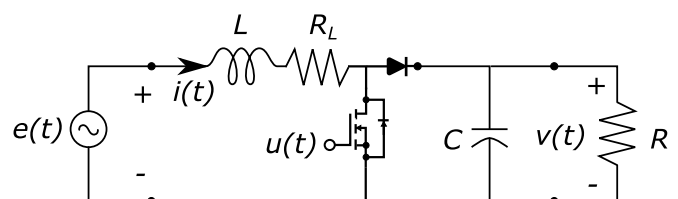


Fig. 1. Simplified Boost converter schematic circuit

The DC-DC boost converter presented in Fig. 1 can be modeled in state-space as proposed in [13] and [14], as

follows:

$$\begin{bmatrix} \frac{di}{dt} \\ \frac{dv}{dt} \end{bmatrix} = \begin{bmatrix} -\frac{R_L}{L} & 0 \\ 0 & -\frac{1}{RC} \end{bmatrix} \begin{bmatrix} i(t) \\ v(t) \end{bmatrix} + \begin{bmatrix} -\frac{v}{L} \\ \frac{i}{C} \end{bmatrix} u(t) + \begin{bmatrix} -\frac{e(t)}{L} \\ 0 \end{bmatrix} \quad (1)$$

In this work, each of the loads are LED strings, and the adaptive controller of the current can control simultaneously the color and the intensity of the lights. Each boost converter can be modeled in discrete time by the following state-space equation

$$\begin{aligned} x[k+1] &= \underbrace{\begin{bmatrix} -a_1 & -a_2 \\ 1 & 0 \end{bmatrix}}_{A_d} x[k] + \underbrace{\begin{bmatrix} 1 \\ 0 \end{bmatrix}}_{B_d} u[k] \\ y[k] &= \underbrace{\begin{bmatrix} b_0 & b_1 \end{bmatrix}}_{C_d} x[k] \end{aligned} \quad (2)$$

The parameters of the state space equation can be estimated adaptive by using the least squares recursive algorithm [15], as follows

$$\theta[k] = \theta[k-1] + M[k](y[k] - \phi^T[k-1]\theta[k-1]) \quad (3)$$

$$P[k] = P[k-1] - M[k]\phi^T[k-1]P[k-1] \quad (4)$$

being $M[k]$ defined as

$$M[k] = \frac{P[k-1]\phi[k-1]}{1 + \phi^T[k-1]P[k-1]\phi[k-1]} \quad (5)$$

and being $\theta[k-1]$ defined as

$$\theta[k] = \begin{bmatrix} a_1 \\ a_2 \\ b_0 \\ b_1 \end{bmatrix} \quad (6)$$

and being $\phi[k-1]$ defined as

$$\phi[k-1] = \begin{bmatrix} -y[k-1] \\ -y[k-1] \\ u[k-1] \\ u[k-2] \end{bmatrix} \quad (7)$$

B. Adaptive Multivariable Decoupled Boost Controller

An adaptive multivariable PID type 2 controller is proposed for control the voltage in each LED string. The PID controller is automatically tuned according to the model parameters estimated by (3) by considering a linear approximated multivariable model. The adaptive capability can track small variations due to the non-linearity and parametric disturbances. The controller is based on a polynomial structure defined by the following equation:

$$E(z) = \frac{c_0z^2 + c_1z + c_2}{(z + c_3)(z - 1)} U(z) \quad (8)$$

being $E(z)$ the \mathcal{Z} transform of the error $e[k] = r[k] - y[k]$, where the resulting control law is defined by:

$$\begin{aligned} e[k] &= -(c_3 - 1)u[k-1] + c_3u[k-2] \\ &+ c_0e[k] + c_1e[k-1] + c_2e[k-2] \end{aligned} \quad (9)$$

By considering (2) and (8) the closed-loop transfer function can be obtained. Thus, by comparing the closed

loop characteristic equation $P_{cl}(z)$ with a desired polynomial $P_d(z)$ defined as follows

$$P_d(z) = z^4 + \alpha_1z^3 + \alpha_2z^2 + \alpha_3z + \alpha_4 \quad (10)$$

the following set of equations are obtained

$$\begin{bmatrix} b_0 & 0 & 0 & 1 \\ b_1 & b_0 & 0 & a_1 - 1 \\ 0 & b_1 & b_0 & a_2 - a_1 \\ 0 & 0 & b_1 & -a_2 \end{bmatrix} \begin{bmatrix} c_0 \\ c_1 \\ c_2 \\ c_3 \end{bmatrix} = \begin{bmatrix} \alpha_1 + 1 - a_1 \\ \alpha_2 + a_1 - a_2 \\ \alpha_3 + a_2 \\ \alpha_4 \end{bmatrix} \quad (11)$$

where the set of equations shown in (11) is solved at each k sample for the parameters identified in (3). This procedure is performed simultaneously for each led string controller.

III. RESULTS

The proposed approach is evaluated in simulation over a single boost converter, and in real time over three boost converters for LED control. In simulation, a boost converter model is used by considering the following parameters: $R = 3\Omega$, $R_L = 1m\Omega$, $L = 250\mu H$, $C = 200\mu F$, $e = 16V$. In Fig. 2 is presented the tracking response by considering the proposed PID type 2 approach.

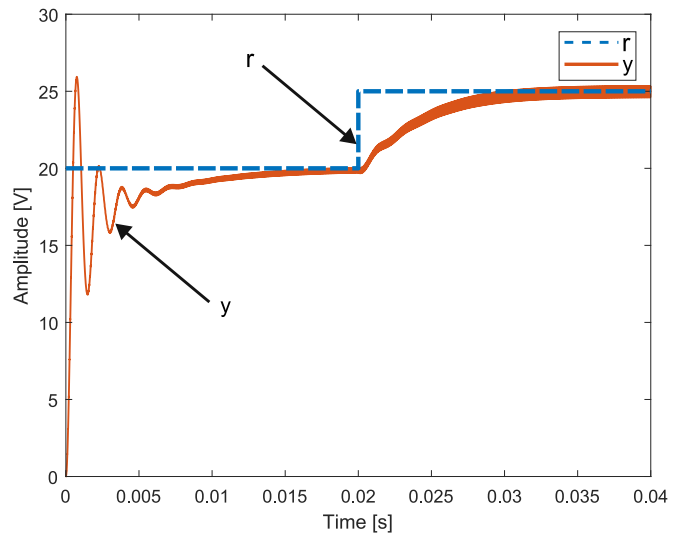


Fig. 2. Reference tracking for the simulated Boost converter

The settling time of the controller is designed for 10 milliseconds without oscillations. In Fig. 2 is shown that the first reference change at time $t = 0$ seconds, exhibits an oscillating behaviour with settling time of 15 milliseconds. This behaviour is due to the identification stage since the system is identified and controlled simultaneously. However, in the second reference change at time $t = 0.02$ seconds, it is shown a settling time of 10 milliseconds and also an output signal without oscillations.

In Fig. 3 is presented the corresponding control signal related to the reference tracking of Fig. 2. It is worth noting that the behaviour of the control signal exhibits some oscillations at time $t = 0$ seconds due to the identification stage, but after that the control signal exhibits a smooth behaviour.

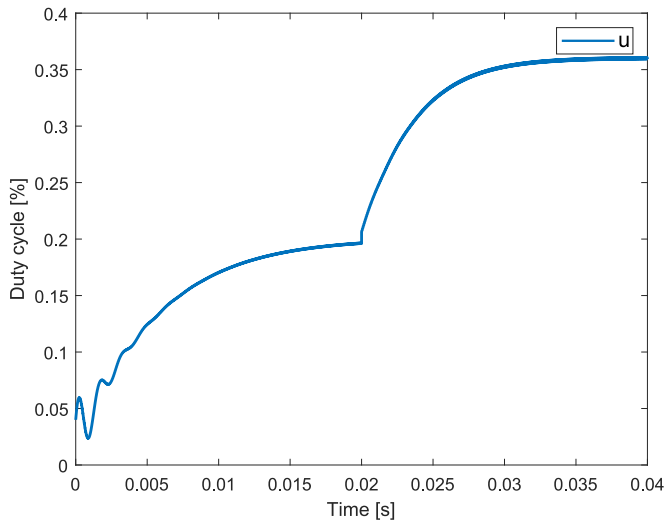


Fig. 3. Duty cycle of the PWM control signal for the simulated Boost converter related to the reference tracking of Fig. 2

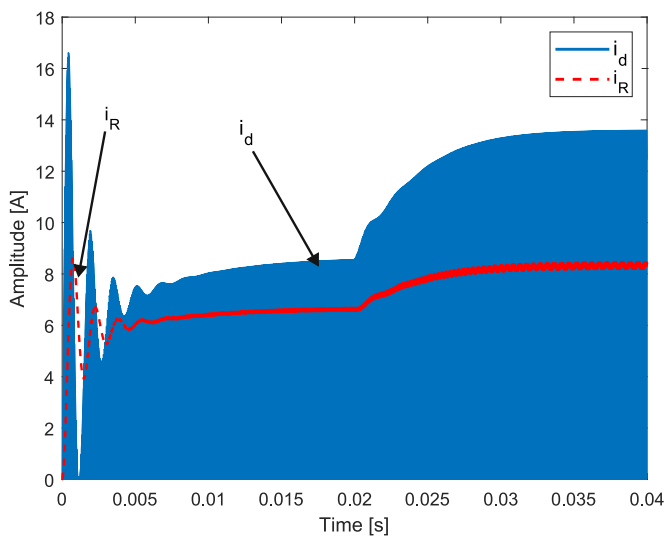


Fig. 4. Switching current at the diode and load current for the simulated Boost converter related to the reference tracking of Fig. 2

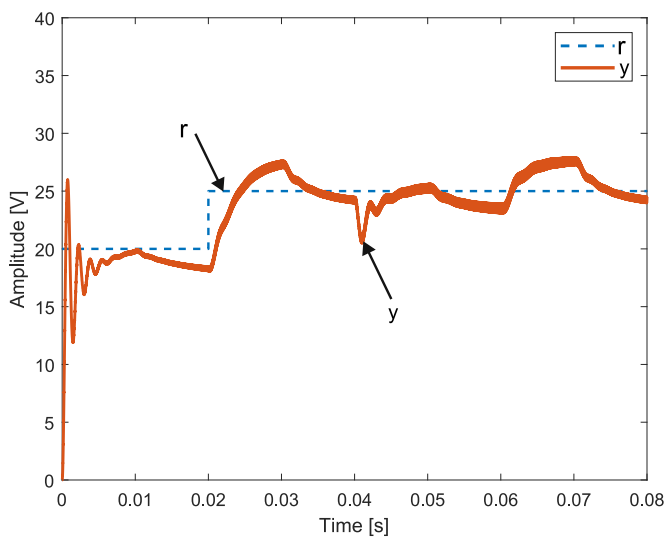


Fig. 5. Reference tracking for the simulated Boost converter by considering a variable input e

In Fig. 4 are presented the switching current at the diode and the current at the load, for the reference tracking of Fig. 2. It is worth mentioning that the behaviour in the first time instants is also consistent with the control signal applied on the boost converter, as shown in Fig. 3. An additional test is performed for a variable voltage input e . In Fig. 5 is shown the reference tracking for the simulated Boost converter by considering a variable input e .

In Fig. 6 is shown the variable input considered for the reference tracking test of Fig. 5.

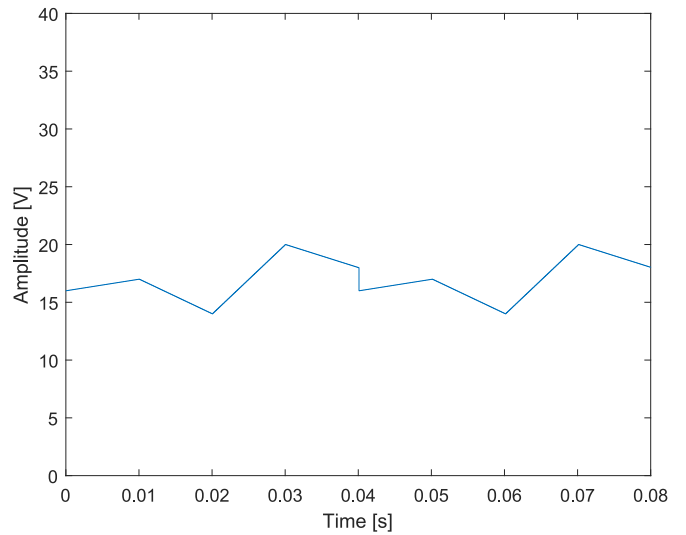


Fig. 6. Variable input e for the simulated Boost converter reference tracking of Fig. 5

In Fig. 7 is presented the corresponding control signal related to the reference tracking of Fig. 5.

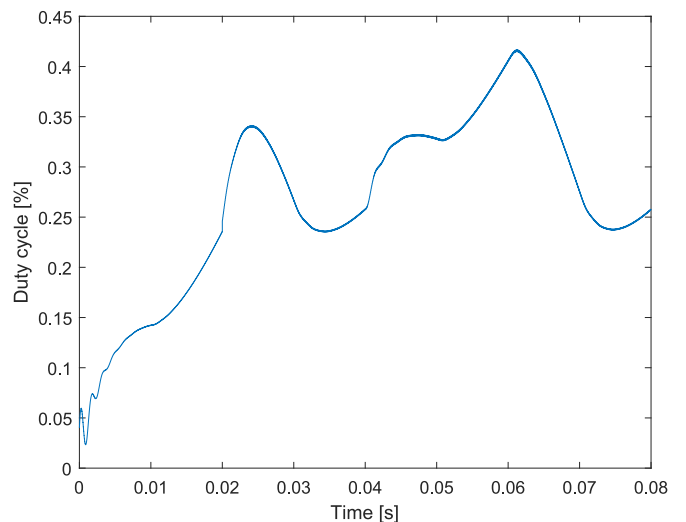


Fig. 7. Duty cycle of the PWM control signal for the simulated Boost converter related to the reference tracking of Fig. 5

In Fig. 8 are presented the switching current at the diode and the current at the load, for the reference tracking of Fig. 5.

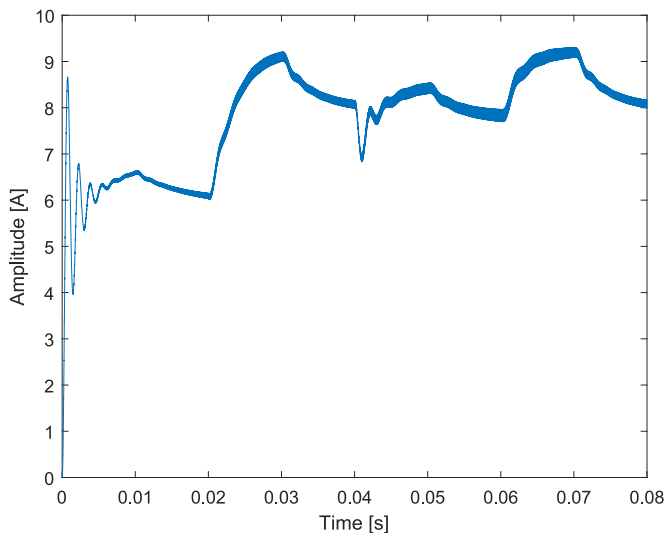


Fig. 8. Switching current at the diode and load current for the simulated Boost converter related to the reference tracking of Fig. 5

The proposed approach is evaluated over three boost converters for LED control, where each LED string contains eight LED of three colors: red, blue and green. To this end, a BOOSTXL-C2KLED board from Texas Instruments is used to evaluate the performance of the controllers, as presented in Fig. 9.

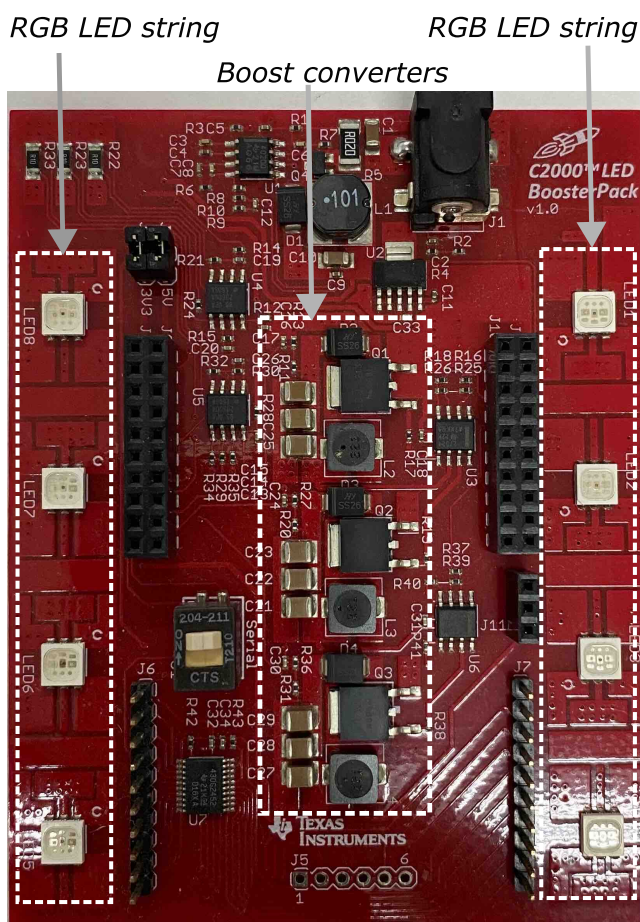


Fig. 9. BOOSTXL-C2KLED boost converter for LED control

The system is connected to a C2000 Delfino F28379D microcontroller, as presented in Fig. 10, in order to write and read the PWM control signals and measured outputs

respectively for each boost converter. It is worth noting that the C2000 Delfino microcontroller has a 200 MHz clock, and the PWM is configured with a $30\mu s$ cycle.

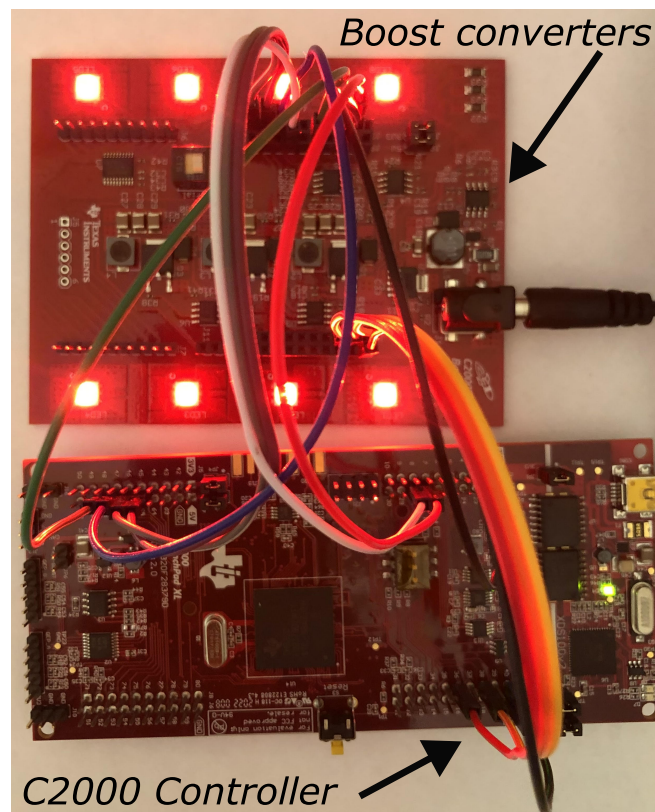


Fig. 10. Boost converter and C2000 microcontroller for LED control

In order to evaluate the performance of the real-time controller over each Boost converter, a 2 channels UNI-T Oscilloscope of 100MHz band-width and 1GS/s sample rate is used. An example of the acquisition of measured current output and PWM input is presented in Fig. 11. However, in order to perform a detailed analysis over the measured input and output data, the acquired signals are transmitted by USB to the computer. The transmitted data corresponding to the Fig. 11 are presented in Fig. 12.

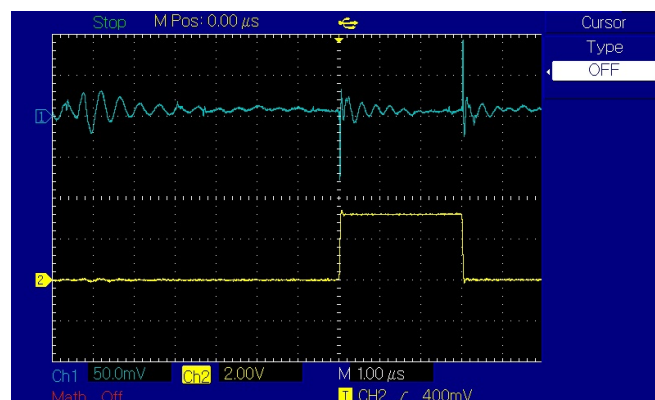


Fig. 11. Open loop response for load current during the application of a PWM pulse in the blue LED string measured by using the oscilloscope

In Fig. 12, a detailed view of the load current and the PWM input shown in Fig. 11 are shown. This result is obtained during the application of a PWM pulse. The system

current output is measured by using an oscilloscope. In Fig. 13, a detailed view of the load current and the PWM input for a step input is presented. In Fig. 14, a detailed view of the load current and the PWM input for a impulse input is presented.

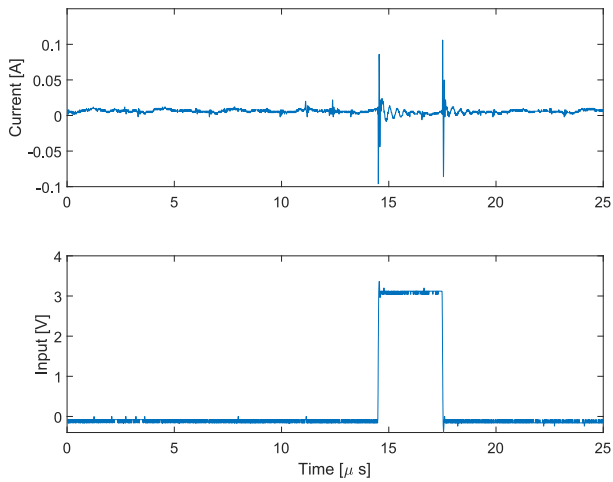


Fig. 12. Detailed current open loop response during the application of a PWM pulse in the blue LED string

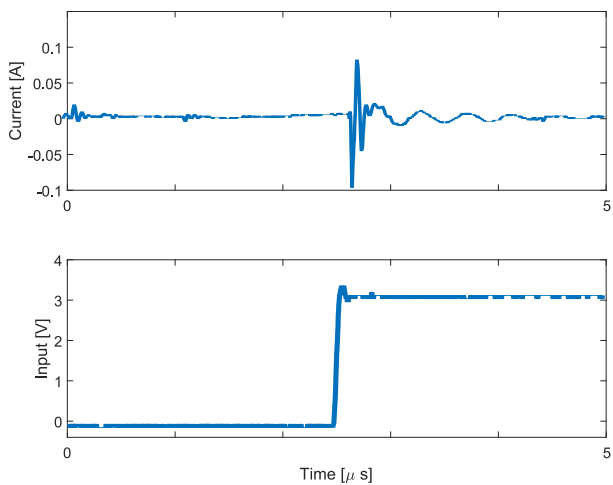


Fig. 13. Detailed current open loop response during the application of a PWM step pulse in the blue LED string

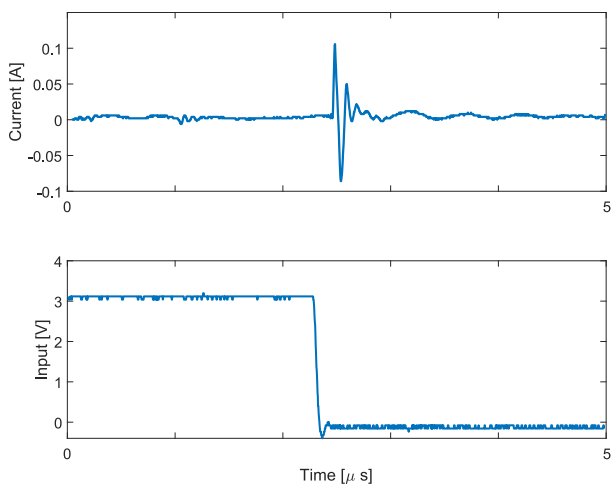


Fig. 14. Detailed current open loop response during the application of a PWM impulse pulse in the blue LED string

In Fig. 15 and Fig. 16, a detailed view of the load current and the PWM input for the boost converter with the red LED string and the green LED string, respectively.

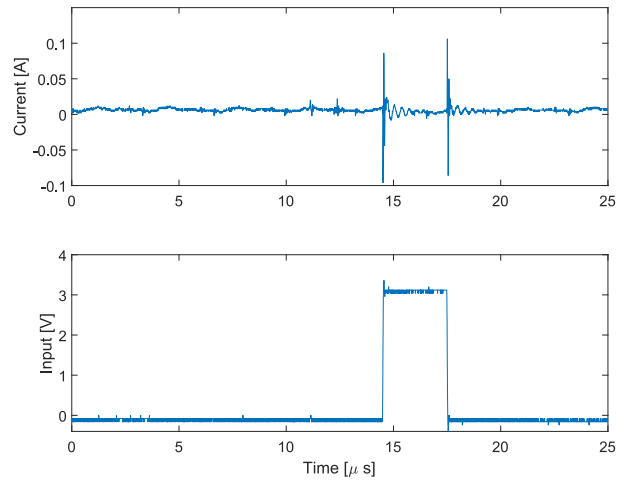


Fig. 15. Detailed current open loop response during the application of a PWM pulse in the red LED string

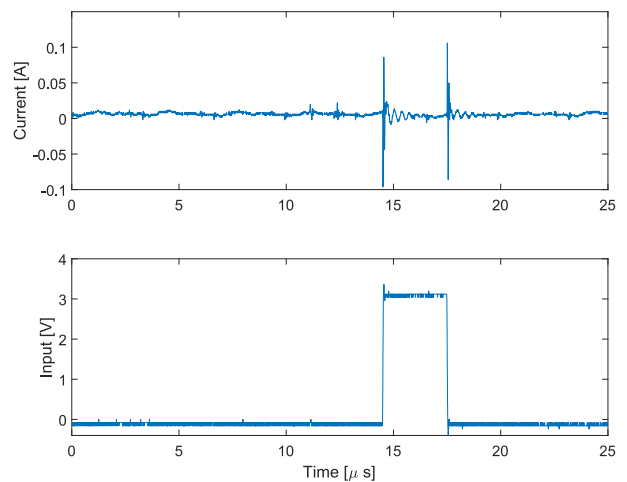


Fig. 16. Detailed current open loop response during the application of a PWM pulse in the green LED string

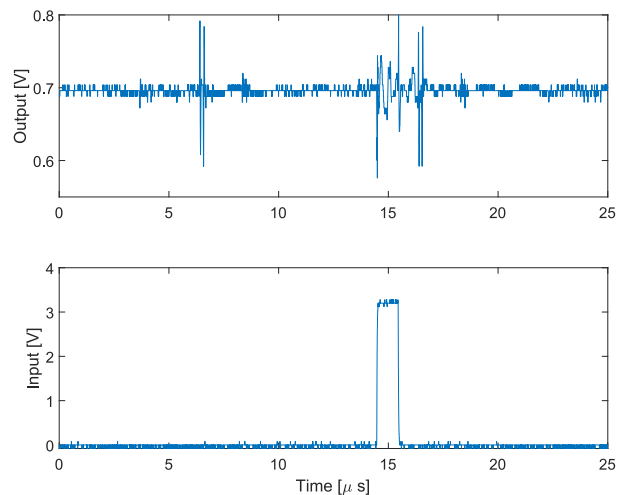


Fig. 17. Detailed voltage open loop response during the application of a PWM pulse in the blue LED string

In Fig. 17, a detailed view of the voltage and the input can be observed during the application of a PWM pulse. The system current voltage is measured by using the oscilloscope.

In Fig. 18, an open voltage output can be observed for 0.6, 0.4 and 0.2 duty cycle PWM values applied during 100 milliseconds intervals.

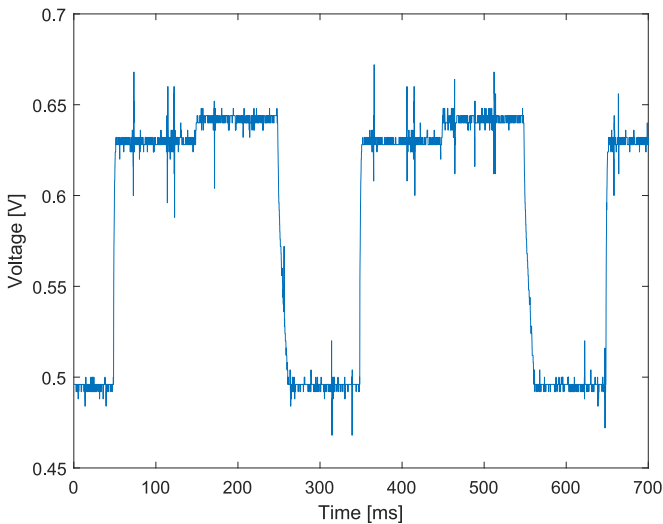


Fig. 18. Open loop voltage output for 0.6, 0.4 and 0.2 PWM values

From Fig. 18 it can be seen that the boost converter achieves a fast steady-state output for 0.6, 0.4 and 0.2 PWM values.

A closed loop voltage response is observed in Fig. 19 for reference tracking for the blue LED string. In this case the reference values are modified every 100 milliseconds, and the voltage output signal effectively track the reference voltage. In this case, a 700 milliseconds window analysis is performed.

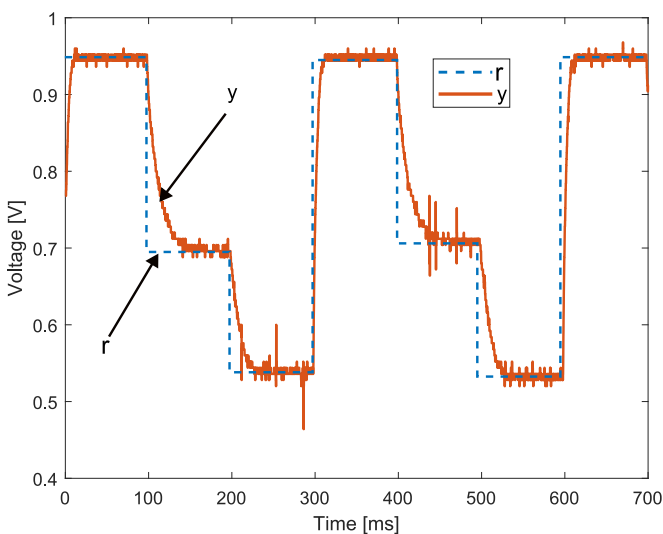


Fig. 19. Closed loop voltage output

A detailed analysis of the closed-loop voltage control is performed, as shown in Fig. 20.

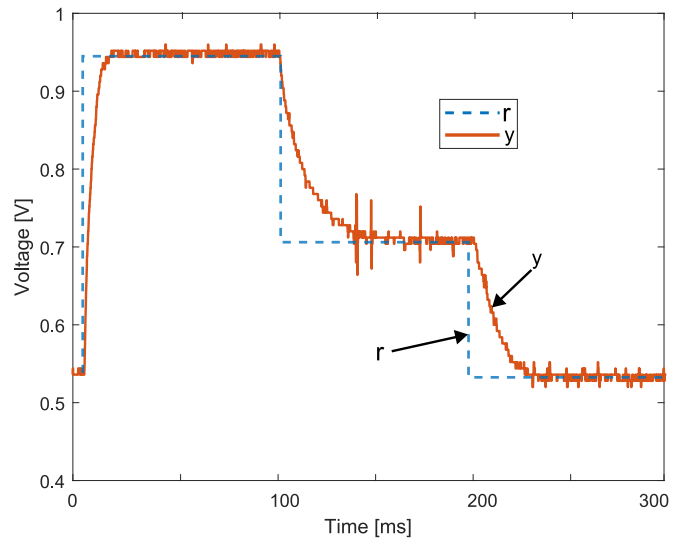


Fig. 20. Closed loop voltage output zoom

IV. CONCLUSIONS

An embedded real-time PID type 2 adaptive controller is proposed for three boost converters connected to three LED strings. It can be seen that the voltage control of the LEDs adequately tracks any Red-Green-Blue (RGB) combination, as a reference signal, by applying an online identification stage. As shown in the results section, the proposed adaptive LED control system simultaneously identifies and controls each led string, resulting in a multivariable decoupled adaptive controller. As described in the results section, the proposed controller is evaluated in real-time over three boost converters using the BOOSTXL-C2KLED system and a LAUNCHXL-F28379D microcontroller from Texas Instruments. A detailed analysis of tracking error and settling time is presented for the embedded controller, where the duty cycle and the corresponding current are also measured. An additional validation over a simulated boost converter is also presented by considering fixed and variable inputs. It can be seen that the proposed approach applied over a simulated boost converter also adequately tracks the reference signal even under variable input. An additional analysis of the tracking response is performed for the first time, where the model is being identified and controlled simultaneously, showing that both tasks can be applied simultaneously. In future works, a coupled multivariable controller can be developed by considering an RGB color sensor as the system's output.

REFERENCES

- [1] M. Wendt and J.-w. Andriessse, "Leds in real lighting applications: from niche markets to general lighting," in *Conference Record of the 2006 IEEE Industry Applications Conference Forty-First IAS Annual Meeting*, vol. 5, 2006, pp. 2601–2603.
- [2] C. Branas, F. J. Azcondo, and J. M. Alonso, "Solid-state lighting: A system review," *IEEE Industrial Electronics Magazine*, vol. 7, no. 4, pp. 6–14, 2013.
- [3] P.-J. Liu, S.-R. Hsu, C.-W. Chang, C.-Y. Liao, and L.-H. Chien, "Dimmable white led driver with adaptive voltage feedback control," in *2015 IEEE 2nd International Future Energy Electronics Conference (IFEEC)*, 2015, pp. 1–4.
- [4] W.-K. Lun, K. H. Loo, S.-C. Tan, Y. M. Lai, and C. K. Tse, "Bilevel current driving technique for leds," *IEEE Transactions on Power Electronics*, vol. 24, no. 12, pp. 2920–2932, 2009.

- [5] J. S. Velez-Ramirez, L. A. Rios-Norena, and E. Giraldo, "Buck converter current and voltage control by exact feedback linearization with integral action," *Engineering Letters*, vol. 29, no. 1, pp. 168–176, 2021.
- [6] M. Bueno-Lopez and E. Giraldo, "Real-time fractional order pi for embedded control of a synchronous buck converter," *Engineering Letters*, vol. 29, no. 3, pp. 1212–1219, 2021.
- [7] E. Giraldo, "Real-time modified pid controller over a dc-dc boost converter," *IAENG International Journal of Applied Mathematics*, vol. 51, no. 4, pp. 892–898, 2021.
- [8] J. S. Velez-Ramirez, M. Bueno-Lopez, and E. Giraldo, "Adaptive control approach of microgrids," *IAENG International Journal of Applied Mathematics*, vol. 50, no. 4, pp. 802–810, 2020.
- [9] A. Marin-Hurtado, A. Escobar-Mejia, and E. Giraldo, "Model reference adaptive multivariable control of a four-leg converter," *Engineering Letters*, vol. 30, no. 3, pp. 1157–1165, 2022.
- [10] J. B. Renteria-Mena and E. Giraldo, "Real-time adaptive level control of a multivariable waste water treatment plant," *Engineering Letters*, vol. 30, no. 3, pp. 444–452, 2022.
- [11] E. Giraldo, "Adaptive indirect field oriented linear control of an induction motor," *IAENG International Journal of Applied Mathematics*, vol. 52, no. 1, pp. 18–23, 2022.
- [12] H. Sira-Ramirez, R. Marquez, F. Rivas-Echeverria, and O. Llanes-Santiago, *Control de Sistemas No Lineales*. Prentice-Hall, Pearson Education, 2004.
- [13] R. H. Tan and L. Y. H. Hoo, "Dc-dc converter modeling and simulation using state space approach," in *2015 IEEE Conference on Energy Conversion (CENCON)*, 2015, pp. 42–47.
- [14] F. F. Valderrama, H. Moreno, and H. M. Vega, "Análisis, simulación y control de un convertidor de potencia dc-dc tipo boost," *Ingenium*, vol. 12, no. 24, pp. 44–55, 2011.
- [15] F. Osorio-Arteaga, J. J. Marulanda-Durango, and E. Giraldo, "Robust multivariable adaptive control of time-varying systems," *IAENG International Journal of Computer Science*, vol. 47, no. 4, pp. 605–612, 2020.